Evol Ecol (2013) 27:353–380
DOI 10.1007/s10682-012-9594-y

ORIGINAL PAPER

The influence of host demography, pathogen virulence, and relationships with pathogen virulence on the evolution of pathogen transmission in a spatial context

Susanna M. Messinger · Annette Ostling

Received: 22 December 2011 / Accepted: 25 June 2012 / Published online: 2 August 2012

Abstract A major challenge in evolutionary ecology is to explain extensive natural variation in transmission rates and virulence across pathogens. Host and pathogen ecology is a potentially important source of that variation. Theory of its effects has been developed through the study of non-spatial models, but host population spatial structure has been shown to influence evolutionary outcomes. To date, the effects of basic host and pathogen demography on pathogen evolution have not been thoroughly explored in a spatial context. Here we use simulations to show that space produces novel predictions of the influence of the shape of the pathogen's transmission–virulence tradeoff, as well as host reproduction and mortality, on the pathogen's evolutionary stable transmission rate. Importantly, non-spatial models predict that neither the slope of linear transmission–virulence relationships, nor the host reproduction rate will influence pathogen evolution, and that host mortality will only influence it when there is a transmission–virulence tradeoff. We show that this is not the case in a spatial context, and identify the ecological conditions under which spatial effects are most influential. Thus, these results may help explain observed natural variation among pathogens unexplainable by non-spatial models, and provide guidance about when space should be considered. We additionally evaluate the ability of existing analytical approaches to predict the influence of ecology, namely spatial moment equations closed with an improved pair approximation (IPA). The IPA is known to have limited accuracy, but here we show that in the context of pathogens the limitations are substantial: in many cases, IPA incorrectly predicts evolution to pathogen-driven extinction. Despite these limitations, we suggest that the impact of ecology can still be understood within the conceptual framework arising from spatial moment equations, that of "self-shading'', whereby the spread of highly transmissible pathogens is impeded by local depletion of susceptible hosts.

S. M. Messinger (✉) · A. Ostling
University of Michigan, 2004 Kraus Natural Science Building, 830 North University, Ann Arbor, MI 48103, USA
e-mail: susmess@umich.edu

A. Ostling
e-mail: aostling@umich.edu

Keywords Spatial structure · Pathogen evolution · Pair approximation · Host ecology · Transmission–virulence tradeoff

Introduction

A significant challenge in disease ecology is to explain the tremendous natural variation in pathogen transmission and virulence across pathogen species. A potentially important source of variation is host and pathogen ecology. For example, the tuberculosis pathogen (*Mycobacterium tuberculosis*) is highly virulent (causes high host mortality) while pneumonia (*Mycoplasma pneumoniae*) is much less virulent (Walther and Ewald 2004). One possible explanation is that the bacteria causing tuberculosis can survive upwards of 250 days in the environment while the bacteria causing pneumonia can survive less than 2 days in the environment (Bonhoeffer et al. 1996; Walther and Ewald 2004). Thus, the negative impact of virulence on pathogen fitness, mediated by host mortality, is less for tuberculosis than pneumonia. The evolutionary importance of environmental pathogen transmission has been more generally addressed in the literature (e.g., Roche et al. 2011; Gandon 1998; Day 2002). Other highly cited ecological explanations for observed variation in pathogen transmission and virulence include the presence and shape of a transmission–virulence tradeoff (Levin and Pimentel 1981; Anderson and May 1982; May and Anderson 1982), the timing of transmission (Cooper et al. 2002; Day 2003; Osnas and Dobson 2010), the mode of transmission (Ewald 1987, 1998; White et al. 2002), and the occurrence of co-infection or super-infection (Levin and Pimentel 1981; Bull 1994; Levin and Bull 1994; van Baalen and Saebelis 1995; Frank 1996; Mosquera and Adler 1998; Nowak and Sigmund 2002; Alizon and Lion 2011).

Our current understanding of the evolutionary influence of host and pathogen ecology is largely based on analysis of mathematical models or inference from observational studies (e.g., Ewald 1993). Empirical studies are limited by the difficulty of isolating the evolutionary influence of one particular ecological factor on pathogen variation. As methods in the study of evolutionary ecology become more sophisticated, observational and theoretical predictions are increasingly being tested (e.g., de Roode et al. 2008; Eshelman et al. 2010). Yet the mathematical theory being tested has been developed primarily from analysis of non-spatial pathogen-host models. Recent theoretical work suggests that spatial context can strongly influence the evolution of interacting species (Johnson and Seinen 2002; Le Galliard et al. 2003; Hansen et al. 2007; Prado and Kerr 2008), including pathogens (Boots and Sasaki 1999; Haraguchi and Sasaki 2000; Rauch et al. 2002; Kerr et al. 2006; Kamo et al. 2007; Lion and van Baalen 2008; Messinger and Ostling 2009; Boerlijst and van Ballegooijen 2010). This is especially relevant for pathogens since host populations are often naturally structured by intrinsic limitations on movement, ranging from immobility (e.g., plants) to restricted home ranges (e.g., many mammal species).

While some theoretical work has addressed the evolutionary impact of host and pathogen ecology in a spatial context (Claessen and de Roos 1995; Boots et al. 2004; Kamo and Boots 2004; Caraco et al. 2006; Kamo et al. 2007), the impact of basic host demography on the evolution of pathogen transmission has not been thoroughly explored. Furthermore, we have only pieces of the whole picture regarding the impact of the shape of the relationship between the pathogen's transmission rate and virulence in a spatial context (see: Boots and Sasaki 1999; Haraguchi and Sasaki 2000; Kamo et al. 2007). In particular, lacking is a systematic exploration of the pathogen's ES transmission rate across both host

demography, relationships between the pathogen's transmission and virulence, and pathogen virulence when there is no transmission–virulence relationship. Given that these aspects of ecology are fundamental to hosts and their pathogens, elucidating their effects in a spatial context may improve our understanding of trait variation across of a broad range of pathogen species.

Here we evaluate via simulations the predicted effect of the shape of the pathogen's transmission-virulence relationship on the pathogen's evolutionary stable (ES) transmission rate. In addition, we evaluate the predicted effect of the host reproduction rate, host natural death rate, and pathogen virulence on the pathogen's ES transmission rate for no transmission–virulence relationship and across a range of linear and concave-down transmission–virulence relationships. We find that the ecological context set by these traits is an important determinant of the pathogen's ES transmission rate even when the non-spatial model predicts they are not. Particularly important is host reproduction: high host reproduction leads to a higher ES transmission rate. In most cases, host death increases the ES transmission rate, but at high host reproduction rates the ES transmission rate can actually decline. Though in some cases the spatial and non-spatial models predict the same qualitative trends with ecology, the quantitative difference varies. In some ecological contexts the quantitative differences are substantial, suggesting that despite overarching qualitative consistency in the theoretical predictions of spatial and non-spatial models, the potential evolutionary effects of spatial structure should not be ignored.

Given the potential of these results to inform our understanding of pathogen evolution, as well as the computational difficulties associated with deriving them for all possible ecological contexts, we additionally evaluate the ability of existing analytical approaches to predict them. Researchers have debated about the best way to quantify pathogen fitness in space and thus predict the evolutionary influence of the ecological context (Slobodkin 1974; van Baalen and Rand 1998; Boots and Sasaki 1999, e.g., compare interpretations of pathogen fitness in: Johnson and Boerlijst 2002; Kerr and Godfrey-Smith 2002; and Rauch et al. 2002, also see: Goodnight et al. 2008). A recent key approach has been to quantify pathogen fitness through the use of spatial moment equations: coupled equations that describe the mean density and spatial arrangement of hosts in a population. These equations enable one to deconstruct fitness into its spatial and non-spatial components and thus more clearly understand how spatial structure will influence the evolution of a particular trait as well as the effect of different ecological contexts. In particular, these equations have highlighted the evolutionary role of "self-shading", when the growth of cheaters or over-exploiters is hindered by the depletion of local resources, and host demography (Boots and Sasaki 1999; Lion and Boots 2010).

Although conceptually insightful, the tractability of the fitness concept based on spatial moment equations depends on the use of a moment closure method. A frequently used method is a pair approximation (PA) (see Boots and Sasaki 2000; Caraco et al. 2006; Kamo and Boots 2006; Kamo et al. 2007) that eliminates the infinite array of moments above pairs of individuals (Matsuda et al. 1992; Harada and Iwasa 1994; Sato et al. 1994). Though it is common knowledge that pair approximations are not always accurate, it is not clear to what extent for host-pathogen interactions. A few recent studies have questioned the accuracy of the PA in predicting the pathogen's ES transmission rate when the pathogen is not subject to a transmission–virulence relationship (de Aguiar et al. 2004; Boots et al. 2006; Lion and Boots 2010), demanding a more comprehensive evaluation.

Here we evaluate the ES transmission rate predicted using the improved pair approximation (IPA), which has commonly been used in studies of spatial pathogen-host dynamics, in comparison to that predicted by spatial simulations. We find that predictions

based on IPA can be qualitatively incorrect, and fail to the largest degree when the effects of spatial structure are most significant. This demonstrates the previously unknown extent of the limitations of IPA in predicting the effect of spatial structure on pathogen evolution and advocates examination of the accuracy of other moment closure methods (e.g., Filipe and Maule 2003; Bauch 2005; Peyrard et al. 2008). However, despite the limitations of the IPA, we find that the relationships with host and pathogen demography uncovered through simulation can still be conceptually understood within the framework of "self-shading". We suggest that future work should explore new constructs for quantifying the effects of "self-shading".

Non-spatial model and predictions

A standard non-spatial model of susceptible-infected host-pathogen dynamics is given by the following equations:

$$\frac{dS}{dt} = (r - d) \cdot S - \beta \cdot S \cdot I \tag{1}$$

$$\frac{dI}{dt} = \beta \cdot S \cdot I - (d + \alpha) \cdot I \tag{2}$$

In this model, S is the number of susceptible hosts, I is the number of infected hosts, d is the host natural death rate, r is the host reproduction rate, β is the infection rate per infected individual, and α is the pathogen virulence (the death rate of the host due to infection). The product of β and I is the infection rate. Thus, $\beta \cdot S \cdot I$ is the number of susceptible hosts that become infected per time assuming complete mixing of the host population. This model assumes that infected hosts do not recover from infection but are removed from the population due to natural death or disease-induced death. A number of real pathogen-host systems conform to this assumption, ranging from very virulent pathogens like lethal yellowing disease to nearly avirulent pathogens like Herpes. The model also assumes that hosts cannot be co-infected. As mentioned, co-infection has been shown to play an important role in pathogen evolution (Levin and Pimentel 1981; Bull 1994; Levin and Bull 1994; Frank 1996; Mosquera and Adler 1998; Nowak and Sigmund 2002). Here, however, our goal is to more carefully explore the role of a limited set of basic host and pathogen ecology related only to demography. As such, we choose to build from a simple model that does not include evolutionary complexities like co-infection.

From the above model, a pathogen's per-capita growth rate is

$$\frac{1}{I} \cdot \frac{dI}{dt} = \beta \cdot \left(S - \frac{d + \alpha}{\beta} \right) \tag{3}$$

where S is the number of susceptible hosts experienced by the pathogen. Given some number of susceptible hosts, the per-capita growth rate decreases with infected host mortality and increases with transmission. The quantity $(d + \alpha)/\beta$ has special significance: it is the expected equilibrium number of susceptible hosts in a monomorphic population, S^*. Thus, the pathogen's per-capita growth rate can be re-written as

$$\frac{1}{I} \cdot \frac{dI}{dt} = \beta \cdot (S - S^*) \tag{4}$$

and the pathogen population is predicted to grow if the actual number of susceptible hosts it experiences is greater than the number expected at equilibrium. S^* is the inverse of the

pathogen's epidemiological R_0 (the number of secondary infections caused per infected individual over its infectious period in a completely susceptible population; Eq. 5).

$$R_0 = \frac{\beta}{d + \alpha} \tag{5}$$

To understand the evolutionary dynamics predicted by this model, we consider the per-capita growth rate of a pathogen from rarity in a dimorphic population, where the host population is already at equilibrium with a resident pathogen strain. In this scenario, both pathogens experience the same actual number of susceptible hosts (S from Eq. 4), which is the number of susceptible hosts at equilibrium with the resident pathogen. Thus,

$$\frac{1}{I_{invader}} \cdot \frac{dI_{invader}}{dt} = B_{invader} \cdot \left[S^*_{resident} - S^*_{invader}\right] \tag{6}$$

If the invader's expected equilibrium number of susceptible hosts in a monomorphic population ($S^*_{invader}$) is less than the actual number it experiences ($S^*_{resident}$, which is also the expected equilibrium number of susceptible hosts in a monomorphic population with just the resident), the invasion will succeed. In terms of R_0, the pathogen with the bigger R_0 can invade. Therefore, this model predicts that selection will maximize R_0. Note that the pathogen's per-capita growth rate is no different if the host is assumed to have logistic rather than exponential growth—the predictions arising from the following invasion analysis are not dependent on any assumptions about the host's growth. This is important since our spatial model effectively regulates the host's growth.

We can understand the non-spatial evolutionary influence of host and pathogen ecology by finding the transmission rate that maximizes R_0 (Eq. 5). Assuming there can be a relationship between the pathogen's transmission rate and virulence ($\alpha = C \cdot \beta^z$), the ES transmission rate that maximizes R_0 is

$$\beta = \sqrt[z]{\frac{d}{C \cdot (z - 1)}} \tag{7}$$

When there is no transmission–virulence relationship ($C = 0$) or if the relationship is linear ($z = 1$), the ES transmission rate is undefined: R_0 is maximized by an infinite transmission rate (and virulence, in the case of a linear transmission–virulence relationship). In practice, the model predicts evolution to pathogen-driven host extinction. Only if there is a transmission–virulence tradeoff ($z > 1$) does the non-spatial model predict an intermediate ES transmission rate. It follows that when there is no transmission–virulence relationship or a linear transmission–virulence relationship, host and pathogen ecology are not predicted to play a role in pathogen evolution. When there is a transmission–virulence tradeoff, the ES transmission rate is predicted to increase with the constant of proportionality (C) and the tradeoff exponent (z). The host reproduction rate is not predicted to influence pathogen evolution when there is a transmission-virulence tradeoff (the parameter r does not even appear in Eq. 7), and the ES transmission rate is predicted to increase with the host natural death rate (d).

Spatial model and predictions

Assuming the same basic susceptible-infected pathogen-host dynamics (no immunity or co-infection), we consider a relatively simple stochastic spatial model where the host

population resides on a regular two-dimensional lattice (150 × 150). Lattice sites can be occupied or empty, hosts are fixed in space, and host reproduction and pathogen transmission only occur between directly adjacent lattice sites. The realized rate of host reproduction is determined by the product of r and the number of empty sites among the host's four nearest-neighboring sites. Similarly, the realized rate of transmission is determined by the product of β and the number of susceptible hosts among the infected hosts four nearest-neighboring sites. Otherwise, the dynamics are as described for the non-spatial model. Though simple, this type of spatial structure captures the key elements of spatially-explicit host-pathogen dynamics and has already been demonstrated to have significant evolutionary effects (Messinger and Ostling 2009). Hence it provides a good starting point for understanding spatial effects on pathogen evolution. Furthermore, this type of spatial structure is potentially representative of several natural host populations, including plants, sedentary plant parasites like aphids and other scale insects, sessile marine animals like barnacles, or animals with limited movement like anemones, starfish, and some terrestrial invertebrates.

Note that in the spatial model, the realized host reproduction rate and pathogen transmission rate differ from the rates quantified by the parameters r and β. The actual parameter value reflects the rate if space were not limiting—in other words, if empty sites for reproduction and susceptible hosts for infection were unlimited. For example, in the absence of the pathogen, a reproduction rate of 25 per host generation yields a realized rate of 3.67 per host generation. This is within the range of measured values of r_{max} for many organisms. Despite the large discrepancy between the actual parameter value and the resulting realized value, the two are always positively related. Thus, the trends in the ES pathogen transmission rate with the actual value reflect the trends with realized value.

To find the ES transmission rate for the spatial model we simulate the dynamics as a Poisson process using the Gillespie algorithm (Gillespie 1977). The algorithm computes the time interval between sequentially occurring events, which is exponentially distributed for a Poisson process. When an event occurs, the probability of a particular event (host birth, host death, and pathogen transmission) is equal to the rate at which that event should occur, divided by the total rate at which events occur. Each time a susceptible host is infected, there is some chance that the infecting strain will mutate and acquire a different transmission rate, slightly different than the parent strain. Starting from a low initial transmission rate, the average transmission rate of the pathogen population changes over time. When the average transmission rate is no longer changing over time, we run the simulation for an additional 2,000 time steps and take the average over the last 2,000 time steps as the ES transmission rate. Although this method has been used elsewhere (e.g., Best et al. 2011), it is different than the method used in other papers (e.g., Kamo et al. 2007, where the ES transmission rate is determined through the outcome of comprehensive pairwise invasions). We compared three different methods of inferring the ES transmission rate and found no difference between them (Appendix 1).

We compare the influence of the shape of the transmission virulence relationship, the host reproduction rate, the host death rate, and the pathogen virulence predicted by the spatial model with the influence predicted by the non-spatial model. We make comparisons for the following cases: no transmission virulence relationship, three types of linear relationships ($\alpha = \beta/3$, $\alpha = \beta/6$, and $\alpha = \beta/10$), and four types of tradeoffs ($\alpha = \beta^{1.1}/10$, $\alpha = \beta^{1.3}/10$, $\alpha = \beta^{1.5}/10$, $\alpha = \beta^{1.7}/10$). For each relationship, including none, we examine a range of host reproduction rates and natural host death rates. For the case of no transmission–virulence relationship we also examine a range of pathogen virulence. For all cases we also show the extinction threshold transmission rate (above which the endemic

equilibrium is unstable and the pathogen causes host extinction) and invasion threshold transmission rate (below which the endemic equilibrium is unstable and the pathogen cannot invade the host population) predicted from IPA. The thresholds predicted by ordinary and improved PAs have been shown to be qualitatively accurate for the type of dynamics and spatial structure examined here (Boots and Sasaki 2000; Haraguchi and Sasaki 2000; Ohtsuka et al. 2006; Webb et al. 2007a, b).

Shape of the transmission–virulence relationship

Assuming a linear transmission–virulence relationship we corroborate over a much broader parameter space the previous finding (e.g., Kamo et al. 2007) that the spatial model predicts an intermediate ES transmission rate and endemism. We further find that the ES transmission rate declines with increasing values of the constant of proportionality (C in the equation $\alpha = C{\cdot}\beta^z$ when $z = 1$) for both low and high host reproduction rates (Fig. 1a). In other words, steeper linear transmission–virulence relationships lead to lower ES transmission rates. This is perhaps intuitive based on the non-spatial prediction that steeper transmission–virulence tradeoffs lead to a lower ES transmission rate, but demonstrates that spatial structure can induce evolutionary effects where non-spatial models predict none.

Similar to the spatial model, assuming a transmission-virulence tradeoff, the spatial model predicts a decline in the ES transmission rate with the tradeoff exponent (z in the equation $\alpha = C{\cdot}\beta^z$ when $C = 0.1$; Fig. 1b). However, across all tradeoff exponents the

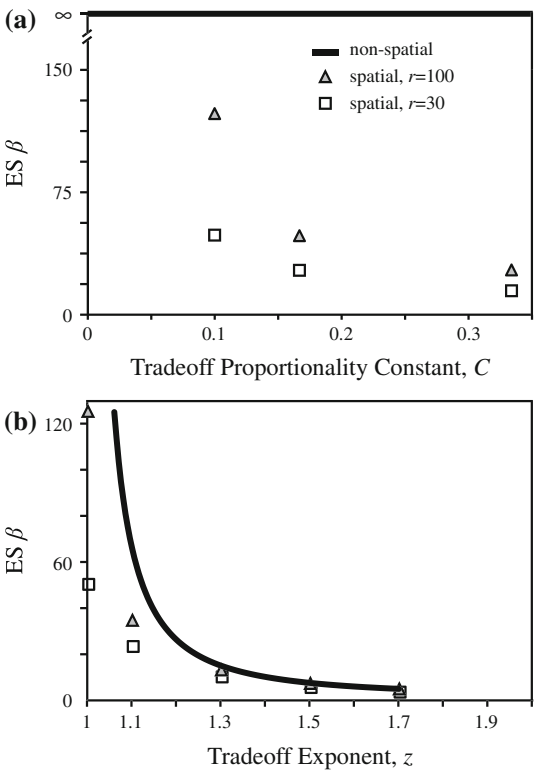

Fig. 1 ES transmission rates across transmission–virulence relationships. The ES transmission rates (ES β) obtained from simulation (data points) and predictions from the non-spatial model (*thick lines*) are shown for different transmission–virulence relationships and for two host reproduction rates ($r = 30$, *squares* and *dashed line*; $r = 100$, *triangles* and *solid line*). **a** Linear transmission–virulence relationships, shape controlled by constant of proportionality C in $\alpha = C{\cdot}\beta^z$ when $z = 1$, **b** concave-down transmission–virulence tradeoffs, shape controlled by tradeoff exponent z in $\alpha = C{\cdot}\beta^z$ when $C = 0.1$

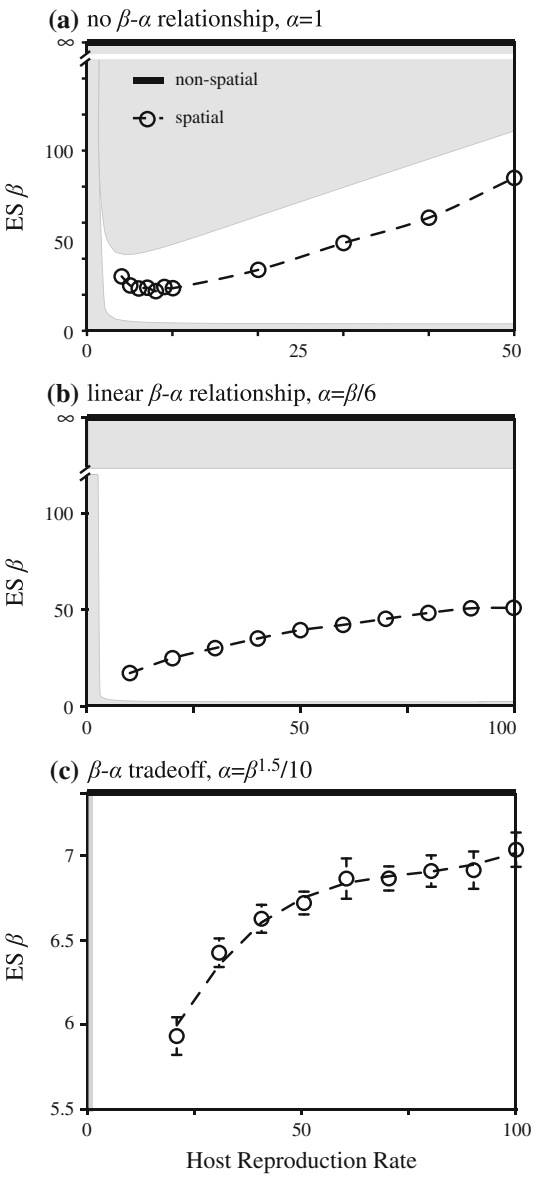

Fig. 2 Effect of host reproduction rate on ES transmission rate. Three examples of the ES transmission rates (ES β) obtained from simulation (data points with *dashed spline fit*) and predictions from the non-spatial model (*thick lines*) across host reproduction rates (r). The *shaded areas are regions* where the IPA predicts extinction of the host, pathogen, or both. In the region to the *left*, the host will go extinct due to an insufficient reproduction rate. In the upper region the pathogen drives the host population and itself to extinction. In the lower region the pathogen cannot invade the host population due to an insufficient transmission rate. In all cases, the non-spatial model predicts no trend with host reproduction rate. **a** no transmission–virulence relationship ($\alpha = 1$), **b** linear transmission–virulence relationship ($\alpha = \beta/6$), and **c** concave-down transmission–virulence tradeoff ($\alpha = 0.1 \cdot \beta^{1.5}$)

spatial ES transmission rate is lower than the non-spatial expectation—a trend that has been hinted at (Messinger and Ostling 2009) but not fully demonstrated.

Host reproduction rate

In contrast to the non-spatial model, for all transmission-virulence relationships including none, the spatial model predicts an intermediate ES transmission rate that varies with the

host reproduction rate (Fig. 2). In particular, assuming no transmission-virulence relationship, the ES transmission rate initially decreases and then increases with host reproduction rate for low host death rates ($d = 1$, $d = 2$) and pathogen virulence ($\alpha = 0$, $\alpha = 1$). For higher host death rates ($d = 3$, $d = 4$) and pathogen virulence ($\alpha = 2$, $\alpha = 3$), the ES transmission rate increases with host reproduction ($d = 1$ and $\alpha = 1$ shown in Figs. 2a, 9). Assuming a transmission–virulence relationship, either linear or a tradeoff, the ES transmission rate increases with the host reproduction rate (Figs. 2b, c, 10, 11). Across all host reproduction rates, the spatial ES transmission rate is always lower than the non-spatial expectation assuming a transmission–virulence tradeoff.

Host mortality

In contrast to the non-spatial model, assuming no transmission–virulence relationship or a linear relationship the spatial model predicts an increase in the ES transmission rate with host death rate (Figs. 3a, b, 12, 13). Assuming no transmission virulence relationship, the spatial model predicts a similar increase with pathogen virulence (Figs. 4, 12). Further, the effect of host death rate and virulence diminishes as host reproduction rate increases, actually reversing at high host reproduction rates such that an increase in host death or virulence decreases the ES transmission rate. In addition, the death rate has a larger effect than the virulence on the spatial ES transmission rate. Finally, the host death rate and virulence most significantly influence evolution assuming no transmission–virulence relationship when host reproduction is low.

Similar to the non-spatial expectation, assuming a transmission–virulence tradeoff the non-spatial model predicts an increase in the ES transmission rate with host death rate across all host reproduction rates (Figs. 3c, 13). However, the non-spatial model consistently predicts a larger increase than the spatial model. In other words, the spatial model predicts a weaker evolutionary effect of the host death rate.

Pair approximation

One way to capture the effects of the type of spatial structure described above is via spatial moment equations that describe the time derivative of paired states on the lattice (Appendix 2). Summing the appropriate state pair derivatives yields the time derivative for infected hosts. From this analysis, a pathogen strain's per-capita growth rate is

$$\frac{1}{I}\cdot\frac{dI}{dt}=\frac{\beta}{n}\cdot\left[Q(S|I)-\frac{d+\alpha}{\beta}\right]=\frac{\beta}{n}\cdot\left[Q(S|I)-Q^{*}(S|I)\right] \tag{8}$$

In this equation, n is the number of lattice sites in the neighborhood of each host (here $n = 4$), $Q(S|I)$ is the actual average number of susceptible hosts in the neighborhood of an infected host, $Q^{*}(S|I)$ is the expected average number at equilibrium in a monomorphic population (which, like S^{*} in the non-spatial model, is the inverse of the pathogen's epidemiological R_0), and all other parameters are as defined for the non-spatial model. Similar to the non-spatial model, the pathogen population is predicted to grow if the actual number of susceptible hosts surrounding an infected host is bigger than the number expected at equilibrium.

As with the non-spatial model, to understand the evolutionary dynamics predicted by the spatial moment equations, we consider the growth rate of a pathogen from rarity in a

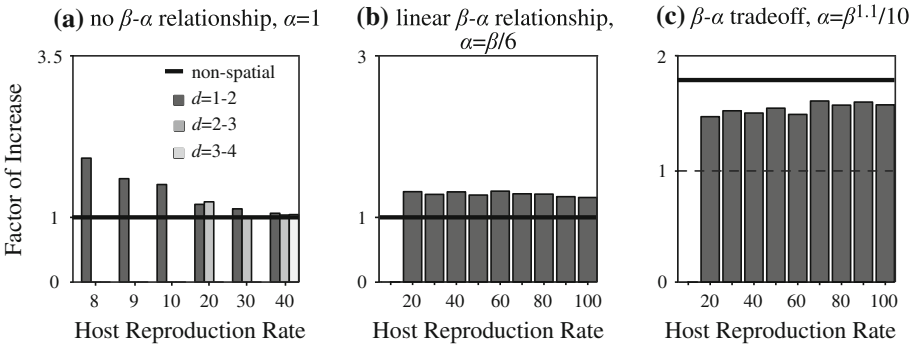

Fig. 3 Effect of host natural death rate on ES transmission rate. Three examples of the factor of increase in the ES transmission rates (ES β) with a unit increase in the host natural death rate (e.g., from $d = 1$ to $d = 2$) obtained from simulation (*bars*) and predictions from the non-spatial model (*thick lines*) across host reproduction rates (r). A factor of increase of 1 represents no change in the ES β with death rate or virulence, a value greater than 1 is an increase, and a value less than 1 is a decrease. For no transmission–virulence relationship and a linear relationship the non-spatial model predicts no change with host natural death rate (factor of increase = 1). **a** no transmission–virulence relationship ($\alpha = 1$), **b** linear transmission–virulence relationship ($\alpha = \beta/6$), and **c** concave-down transmission–virulence tradeoff ($\alpha = 0.1 \cdot \beta^{1.1}$)

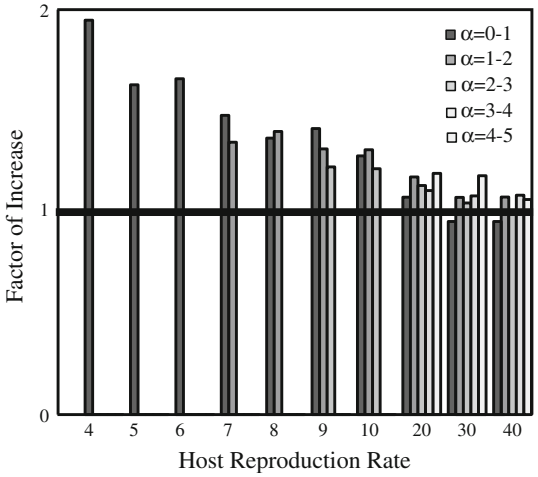

Fig. 4 Effect of virulence on ES transmission rate for no transmission–virulence relationship. An example of the factor of increase in the ES transmission rate (ES β) with a unit increase in the virulence from simulations (*bars*) along with predictions from the non-spatial model (*thick lines*) is shown for a range of host reproduction rates. A value of 1 represents no change in the ES β with death rate or virulence, a value greater than 1 is an increase, and a value less than 1 is a decrease. The non-spatial model predicts no change with pathogen virulence (factor of increase = 1). Other parameters: $d = 1$

dimorphic population, where the host population is already at equilibrium with a resident pathogen strain. If we make the assumption that the resident and invading pathogen experience the same actual average number of susceptible hosts at the time of invasion ($Q(S|I)$ from Eq. 8) and that it is equal to the resident's expected equilibrium value, the invading pathogen's per-capita growth rate is

$$\frac{1}{I_{invader}} \cdot \frac{dI_{invader}}{dt} = \frac{\beta_{invader}}{n} \cdot [Q^*(S|I_{resident}) - Q^*(S|I_{invader})] \quad (9)$$

This leads to an invasion criterion similar to the non-spatial model: if the invader's expected equilibrium average number of susceptible hosts around an infected host in a monomorphic population ($Q^*(S|I_{invader})$) is less than the actual number it experiences ($Q^*(S|I_{resident})$), which is also the expected equilibrium average number in a monomorphic population with the resident), the invasion will succeed. However, in a spatial context the resident and invading pathogen will not experience the same $Q(S|I)$—a rare invading pathogen can have an immediate and large impact on the number of susceptible hosts in its local neighborhood. Therefore, shortly after invasion, the resident pathogen will experience $Q^*(S|I_{resident})$ susceptible hosts but the invading pathogen will experience a quasi-equilibrium number, $Q^0(S|I_{invader})$. At quasi-equilibrium the invading strain is still rare but has come to equilibrium with its local neighborhood (Matsuda et al. 1992). This yields instead

$$\frac{1}{I_{invader}} \cdot \frac{dI_{invader}}{dt} = \frac{\beta_{invader}}{n} \cdot [Q^0(S|I_{invader}) - Q^*(S|I_{invader})] \quad (10)$$

By this equation, the invasion will succeed if $Q^0(S|I_{invader})$ is greater than $Q^*(S|I_{invader})$. Note that even though this representation of the invasion fitness does not explicitly include the resident strain, $Q^0(S|I_{invader})$ depends on how the resident pathogen has already shaped the host population. For example, if there are very few susceptible hosts in the population to begin with, the invader is unlikely to realize a high $Q^0(S|I_{invader})$. In addition, note that Boots and Sasaki (1999) take this one step further to frame the invasion fitness as a balance between the difference in $1/R_0$ of the resident and invader (well-mixed effects) and the difference in $Q(S|I)$ of the resident at equilibrium and invader at quasi-equilibrium (spatial effects). This alternative representation implies that the resident pathogen must be accounted for in ways beyond it's effect on $Q^0(S|I_{invader})$, however, when interactions are completely local, $1/R_0 = Q^*(S|I)$ for the resident and thus cancel out of the equation.

Equation 10 provides a conceptual framework for explaining the effect of spatial structure on pathogen evolution. Because a highly transmissible pathogen quickly infects neighboring susceptible hosts, it will tend to have a lower $Q^0(S|I_{invader})$, thus diminishing its overall ability to invade the population. In effect, highly transmissible pathogens "self-shade" themselves. The risk of "self-shading" will vary depending on the invasion context. For example, if there are many susceptible hosts available upon invasion, the risk is lower than if there are few. An alternative framework for explaining the effect of spatial structure on pathogen evolution has more recently been proposed by Lion and Boots (2010). They derive the selection gradient for the pathogen's transmission rate. In this framework, the risk of "self-shading" also depends on the invasion context: in addition to the density of susceptible hosts around an infected host, it depends on the density of empty sites around an infected host and the relatedness of neighboring pathogens.

Although conceptually insightful, Eq. 10 and the selection gradient formulated by Lion and Boots (2010) are not closed: the average pair densities depend on higher order spatial correlations. For example, the number of susceptible hosts next to infected hosts ($Q(S|I)$) depends on higher order spatial moments (e.g., $Q(S|IS)$). The dependencies continue upward in scale to the size of the entire lattice. Thus, in order to quantify pathogen fitness or the selection gradient, one must use a moment closure method. A simple moment closure method often used is the improved PA (IPA) (Sato et al. 1994). PAs take advantage of the fact that the number of state triples on a lattice can be written in terms of the two

state pairs that it is composed of. If one makes certain assumptions about the distribution of state triples across the lattice (see: Morris 1997), the relationship between state triples and pairs simplifies so that correlations above pairs can be ignored. The IPA is a special PA that accounts for the aggregation of susceptible hosts in space due to local reproduction (Appendix 3).

Here we infer the ES transmission rate predicted by an IPA of the spatial moment equations using Eq. 10. For each transmission-virulence relationship, including none, and parameter set we numerically solve for the quasi-equilibrium $Q(S|I)$ (method described in: Kamo et al. 2007; see Appendix 4) and use it to calculate the invasion fitness for pairs of resident and invading pathogens. The transmission rate of the pathogen that cannot be invaded by any other pathogen strain is taken as the ES transmission rate. To find the predicted extinction threshold transmission rate and the invasion threshold transmission rate, we perform a stability analysis of the endemic equilibrium (methods described in: Sato et al. 1994).

Somewhat surprisingly, we find that like the non-spatial model, assuming no transmission–virulence relationship the IPA predicts evolution to an infinite transmission rate across all host reproduction rates, host death rates, and pathogen virulence. Assuming a linear transmission–virulence relationship, the IPA demonstrates inconsistent qualitative accuracy in predicting the trends between the ES transmission rate and the shape of the transmission–virulence relationship, host reproduction rate, and host death rate. In particular, it is only qualitatively accurate in predicting the effect of the shape of the transmission–virulence relationship and can be quite inaccurate in predicting the trends with host reproduction rate and host death rate (for example, see Fig. 5). Finally, assuming a transmission–virulence tradeoff, the IPA demonstrates consistent qualitative accuracy in predicting the trends between the ES transmission rate and host and pathogen demography. However, we note that the quantitative accuracy varies, in some cases by more than an order of magnitude. For a full summary of the accuracy of the IPA, see Appendix 5.

Discussion

Effects of host and pathogen ecology

Through extensive spatially-explicit simulations of host–pathogen interactions and comparison with non-spatial theory, we identified novel ways in which host and pathogen ecology can influence the pathogen's ES transmission rate in a spatial context. In particular, we have shown that in a spatial context: (1) the shape of the transmission-virulence relationship is important even when it is not an explicit tradeoff, (2) the host reproduction rate plays an important evolutionary role, and (3) host mortality has a broader influence than expected in a non-spatial context (and can even have an influence opposite to that predicted by non-spatial models). In addition, for ecological contexts where the spatial and non-spatial models yield qualitatively consistent predictions, we have identified when space is still likely to have strong quantitative effects.

First, in contrast to non-spatial expectations, we found that in a spatial context the slope of the linear transmission–virulence relationship strongly influences the ES transmission rate: as the relationship becomes steeper, the ES transmission rate decreases. These results suggest that when the host population is spatially structured, the details of the transmission-virulence relationship can be important even when that relationship is not an explicit tradeoff. Space seems to induce an *effective* tradeoff between transmission and virulence

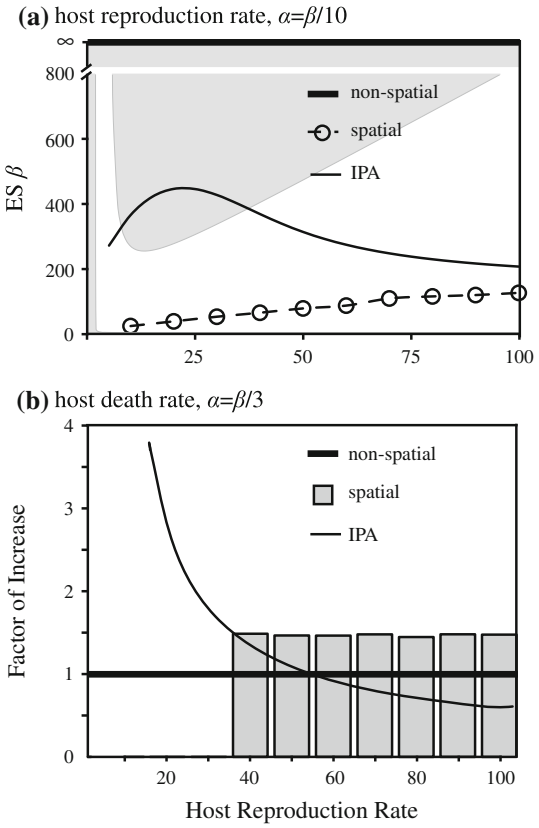

Fig. 5 Trends with host ecology predicted by IPA. **a** An example of the ES transmission rate (ES β) predicted by the improved pair approximation (IPA; *thin line*) compared with predictions obtained from simulation (*circles* with *dashed spline fit*) and the non-spatial model (*thick line*) for a linear transmission-virulence relationship ($\alpha = 0.1 \cdot \beta$) across host reproduction rates (r). The *shaded areas* are as in Fig. 2. Notably, for low host reproduction rates the IPA predicts an ES β that is in the region of pathogen-driven extinction and is furthermore qualitatively different than predicted by simulations. **b** An example of the factor of increase in the ES transmission rate (ES β) with a unit increase in the host natural death rate predicted by the improved pair approximation (IPA; *thin line*) compared with predictions from simulations (*bars*) and the non-spatial model (*thick line*) for a linear transmission–virulence relationship ($\alpha = \beta/3$) across a range of host reproduction rates (r). A value of 1 represents no change in the ES β with death rate or virulence, a value greater than 1 is an increase, and a value less than 1 is a decrease. The IPA predicts a qualitatively different trend than predicted by simulations

even when the direct relationship between these traits is only linear. Furthermore, although when the relationship is a tradeoff the influence of the shape of the tradeoff on the ES transmission rate is qualitatively similar in a spatial and non-spatial context (the ES transmission rate declines with increasing tradeoff steepness), the quantitative difference between the spatial and non-spatial prediction increases and becomes substantial as the tradeoff gets shallower and as the host reproduction rate increases. These results imply that for pathogens with a shallow transmission–virulence tradeoff, consideration of space is particularly important for fully understanding pathogen evolution.

Second, we have shown that in space the ES transmission rate is influenced by the host reproduction rate, whereas in a non-spatial context it is predicted to have no influence. In

particular, when the pathogen is subject to a transmission-virulence relationship, the ES transmission rate increases with the host reproduction rate. This trend was postulated based on other studies (Messinger and Ostling 2009; Lion and Boots 2010) but was not comprehensively tested. In the case of no transmission-virulence relationship, we show that the ES transmission rate decreases then increases with host reproduction across a wide range of host death rates and virulence. This trend was previously shown only for one set of parameter values ($\alpha = 1$, $d = 1$; Haraguchi and Sasaki 2000). When there is no transmission-virulence relationship, the ES transmission rate approaches the pathogen-driven extinction threshold at low and high host reproduction rates. Notably, the non-spatial model predicts that the host reproduction rate will not influence pathogen evolution, regardless of the presence or shape of a transmission–virulence relationship. Thus, a more complete theory of pathogen evolution that considers the influence of space, predicts that existing variation in pathogen transmission rates may arise from differences in the intrinsic host reproduction rate.

Third, we find that in a spatial context the ES transmission rate typically increases with the host natural death rate for all transmission–virulence relationships and no relationship, but can actually decline with host death rate for high host reproduction rates in the case of no relationship. Importantly, the non-spatial model predicts that host death rate will influence pathogen evolution only in the case of a transmission–virulence tradeoff, and it never predicts a decline with host death rate. Furthermore, in the case of a transmission–virulence tradeoff, where the spatial and non-spatial models qualitatively agree regarding the influence of the death rate, the non-spatial predicted change in the ES transmission rate with host death is consistently greater than predicted by the spatial model. As host death rates increase, the spatial prediction diverges from the non-spatial prediction and in this sense spatial effects become strong (for example, given $\alpha = 0.1 \cdot \beta^{1.1}$, the spatial ES transmission rate is 66.8 % lower than the non-spatial prediction for $d = 1$ and $r = 20$ but 74.2 % lower for $d = 2$ and $r = 20$).

Interestingly, we also find an important interactive effect between the effects of the host's reproduction and mortality rates. More specifically, for no transmission–virulence relationship or a less steep linear relationship, the spatial model predicts an increase in the ES transmission rate with host mortality (host death rate or virulence) that diminishes with host reproduction. In other words, host mortality has less influence on the evolutionary dynamics as host reproduction increases. This implies that an increased host reproduction rate not only directly influences the ES transmission rate (as seen in Fig. 2) but can also indirectly influence it by moderating the impact of other demographic rates. This is a particularly relevant finding since host reproduction is not predicted to influence pathogen evolution at all in a non-spatial context. The indirect effects of host reproduction do not extend to steeper linear relationships and tradeoffs, where the influence of the host death rate is fairly constant across reproduction rates.

Finally, the spatial model predicts an evolutionary role for the pathogen's virulence that is not predicted by the non-spatial model. For no transmission–virulence relationship, the pathogen virulence increases the ES transmission rate. In contrast, the non-spatial model predicts that pathogen virulence will not influence the ES transmission rate.

Accuracy of the IPA

We demonstrate that the IPA does not always accurately predict the influence of host and pathogen ecology on pathogen evolution in a spatial context. In particular, we confirm for a wide range of host and pathogen ecology what has been hinted at in the literature for a few

cases: the IPA is dramatically inaccurate when the pathogen is not subject to a transmission-virulence relationship, predicting pathogen-driven extinction while the spatial model predicts endemism (de Aguiar et al. 2004; Boots et al. 2006; Lion and Boots 2010). Perhaps more surprising, we show that the same can be true for less steep linear relationships, especially for low host reproduction rates and high host death rates. For steeper linear relationships the IPA correctly predicts endemism. This has previously been shown for similarly steep relationships, including $\alpha = 3{\cdot}\beta$ where $d = 0.01$ and $r = 3$ (Boots and Sasaki 1999; Kamo et al. 2007), as well as for $\alpha = C{\cdot}\beta$ where C ranges from 0.01 to 0.2, $d = 1$, and $r = 8$ (Haraguchi and Sasaki 2000). However, we show that despite correctly predicting endemism, the IPA predicts different qualitative trends with increasing host reproduction and host death rate. Finally, we show that the IPA correctly predicts endemism and qualitatively predicts the correct trends with increasing host reproduction when there is a transmission–virulence tradeoff. However, for less steep tradeoffs, lower host reproduction rates, and higher host death rates, the quantitative difference increases. Notably, these are the same conditions for which the spatial and non-spatial predictions diverge most, meaning that the IPA performs most poorly when spatial structure is most influential.

That the IPA is not always a good predictor of pathogen evolution is not surprising. However, its limitations appear to be more extensive than initially suspected. Especially in cases where the pathogen is not subject to a transmission–virulence relationship or when the relationship is linear and shallow, new analytical methods of quantifying pathogen fitness should be investigated. Forays in that direction have already been made (Filipe and Maule 2003; Bauch 2005; Peyrard et al. 2008) and have shown some success in predicting equilibrium population densities. However, this does not necessarily suggest that these methods will be accurate predictors of evolutionary outcomes, since the improved pair approximation has also been shown to do well predicting equilibrium population densities and stability (Sato et al. 1994; Boots and Sasaki 2000; Haraguchi and Sasaki 2000; Ohtsuka et al. 2006; Webb et al. 2007a, b). A more careful examination of the spatial correlations in the cases where the IPA does not work well might suggest in particular why the IPA fails and inform the development of new methods. For example, Dieckmann and Law (2000) suggest that larger scale spatial structure may be more appropriately modeled with diffusion approximations, which could potentially be combined with moment approximations to more accurately predict spatial effects.

Explaining the effects of ecology

Despite the quantitative limitations of the IPA, we can qualitatively understand the influence of particular aspects of the host and pathogen ecologies on pathogen evolution within the conceptual framework arising from spatial moment equations. The invasion fitness of a pathogen derived from spatial moment equations implicates "self-shading," where the spread of more transmissible pathogens is impeded by the rapid depletion of the local supply of susceptible hosts, as an important evolutionary force in a spatial context. Examination of the spatially-explicit patch structure arising in different ecological contexts alludes to the relationship between "self-shading" and host and pathogen ecology. Consider host reproduction. Regardless of the transmission-virulence relationship, host reproduction increases local host availability. Therefore, when host reproduction is high the risk of "self-shading" is lower, resulting in a higher ES transmission rate. The trend of initially decreasing ES transmission rate with host

reproduction when there is no relationship may arise because when the host reproduction rate is very low, the initial infecting pathogen strain creates a highly depauperate host population. Subsequently, most pathogens quickly go locally extinct but small, uninfected patches of susceptible hosts are free to grow. These patches can get very large before they come into contact with the sparsely occurring infected hosts (Fig. 6). The risk of "self-shading" in these large patches is low. Thus, it is the periodic formation of very large patches of susceptible hosts at lower host reproduction that favors a higher ES transmission rate. This does not occur when the pathogen is subject to a transmission–virulence relationship, most likely because the initial infection does not lead to such a large reduction in susceptible hosts because infected hosts die more quickly (Fig. 6).

The trends with host natural death rate and virulence are not immediately intuitive, but can also be understood within the framework of "self-shading" once the spatially explicit patch structure in different ecological contexts is identified. By reducing the availability of susceptible hosts, one might assume that the host natural death rate would increase the risk of "self-shading" and thus reduce the ES transmission rate. However, empty sites are necessary for host reproduction. Thus, by creating space for new susceptible hosts, an increased host natural death rate may actually increase host availability and thus ultimately

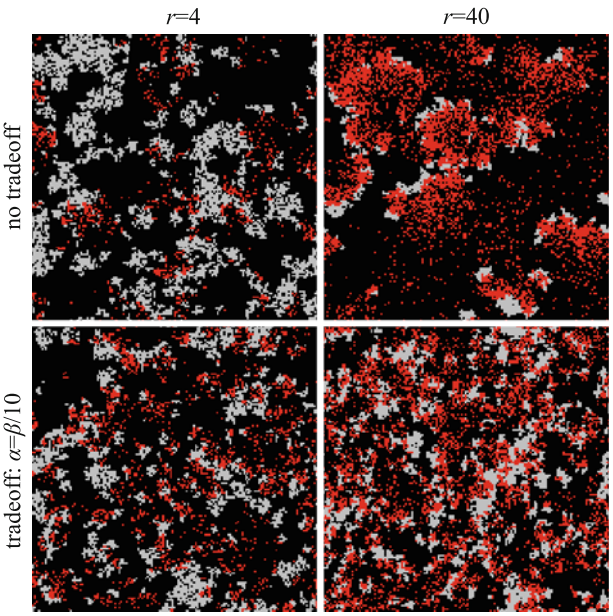

Fig. 6 Population structure for lowest and highest host reproduction rates. Shown is the spatial distribution of empty sites (*black*), susceptible hosts (*gray*), and infected hosts (*red*) for low host reproduction (*left column*) and high host reproduction (*right column*) for no transmission–virulence relationship (*top row*) and a linear relationship of $\alpha = 0.1 \cdot \beta$ (*bottom row*). In case of no relationship, when host reproduction is low, uninfected patches of susceptible hosts grow very large before becoming infected, actually reducing the risk of "self-shading". This does not occur in the linear relationship case. Note that host reproduction is not chosen to be lower in the linear relationship case because the range of transmission rates leading to endemism (between the invasion and extinction threshold transmission rates) is very narrow and due to demographic stochasticity, simulation data could not be obtained. Other parameters: $d = 1$, and for linear relationship $\alpha = 1$

reduce the risk of "self-shading" (for example, the average number of susceptible hosts over 500 time steps during evolutionary equilibrium when there is no transmission–virulence relationship, $r = 10$, $\alpha = 1$, and $d = 1$ is 2,825 ± 264.6 while for $d = 2$ it is 3,999 ± 446.2). In addition, the host natural death rate applies to infected hosts: fewer infected hosts results in lower predation pressure and thus reduces the risk of "self-shading." When there is no transmission–virulence relationship, by removing infected hosts virulence also creates space for new susceptible hosts and reduces the predation pressure. Thus, it similarly affects the ES transmission rate. However, because virulence only affects infected hosts it does not create as much empty space for new susceptible hosts and therefore has less of an effect on the ES transmission rate than the host natural death rate. Further, when host reproduction is high, the benefit of increased host natural death or virulence in terms of empty space relative to the direct cost to the pathogen in terms of decreasing susceptible and infected hosts is lower, potentially explaining the diminishing effect with host reproduction and eventual trend reversal for no transmission–virulence tradeoff.

Summary

In summary, host and pathogen ecology play an important role in the evolution of pathogen transmission rate when the population is spatially structured and may help explain variation among pathogens. We find that when there is no transmission–virulence relationship or when the relationship is linear and less steep, the host reproduction rate is a key determinant of pathogen evolution. Importantly, the non-spatial model predicts that the host reproduction rate should not influence the ES transmission rate. Understanding the effects of basic host demography and pathogen life-history will help to inform our understanding of the problematic emergence and re-emergence of infectious disease and the factors that increase the risk of such events. Although we show that the IPA is not a good method for quantifying "self-shading" and predicting these patterns, most notably in the cases where the effect of spatial structure is strongest, the conceptual framework of "self-shading" is still useful for gaining insights into the role of different ecological contexts. Thus, future work should focus on developing new approximations as well as alternative constructs for quantifying the effects of "self-shading."

Acknowledgments We would like to thank the Associate Editor and the reviewers for their comments and the Rackham Graduate School of the University of Michigan for funding.

Appendix 1

Inferring ES transmission rate from simulations

By definition, the ES transmission rate is the transmission rate that cannot be invaded by any other transmission rate. Using simulations, one can infer the ES transmission rate from the results of a multitude of discrete pair-wise invasions (see for example Kamo et al. 2007). The ability of one pathogen strain to invade another is taken as the average number of successful invasions out of some number of trial invasions. One can also infer the ES transmission rate from the results of continuous invasion by mutation (see for example Webb et al. 2007a, b). Once the pathogen strain with the ES transmission rate invades, no

other mutant strain will be able to invade and the average transmission rate in the population will stabilize at the ES value. The notable, and potentially important difference between the two methods is that the under pair-wise invasion there are never more than two pathogen strains in the population at one time while under continuous invasion many strains are present. To be sure our results were not dependent on our method of inference, we tested three different methods of inferring the ES transmission rate from simulations: pair-wise invasion, continuous invasion by small mutations, and continuous invasion by random mutation.

For the pair-wise invasion method we started the host population with a single resident strain at equilibrium. We then allowed a second pathogen strain with a random transmission rate to invade. Once either the invading or resident strain had been excluded from the host population, the process was repeated. Although this method is not exactly the same as a complete pair-wise invasion analysis, it does capture the essential feature that only two pathogen strains reside in the population at any given time. For the two continuous invasion methods, the ES transmission rate is taken as the average transmission rate of the pathogen population over 2,000 time steps when it is no longer changing over time (a slope between -0.001 and 0.001). For the continuous invasion by random mutation method, we allowed mutant pathogens to differ randomly (rather than only by a small amount) from the parent strain. In all cases, for at least one set of parameters we started the simulation from a range of initial transmission rates. Regardless of the initial transmission rate, the predicted ES transmission rate was the same, suggesting that evolutionary bi-stability is not a fundamental feature of the model.

To determine whether the methods yielded different results, we compared the ES transmission rate across multiple realizations of each method for the case of no transmission–virulence tradeoff. The three methods did not give significantly different predictions (Fig. 7). Thus, using the ES transmission rate predicted by the less computationally intensive continuous evolution method is an accurate comparison point for the ES transmission rate predicted by an IPA of the spatial moment equations.

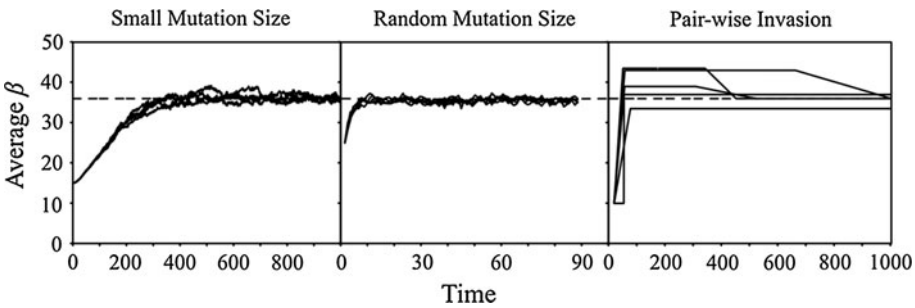

Fig. 7 Comparing methods of inferring evolutionary stable transmission rate (ES β) for no transmission–virulence relationship. The *left panel* shows the average pathogen transmission rate (β) over time for six different stochastic simulations where evolution is modeled as continuous evolution by small mutations. The *middle panel* shows the same for continuous evolution with randomly sized mutations. The *right panel* shows the average β over time for simulations consisting of a sequence of pair-wise invasions—there are only ever two pathogen strains in the population at one time. The *dashed line* shows the ES β inferred by averaging across the last 500 time steps of the continuous evolution by small mutation data. In the analyses here we found no substantial difference in the ES β obtained across these methods. Other parameters are $r = 20$, $\alpha = 1$, and $d = 1$

Appendix 2

Spatial moment equations

On a regular two-dimensional lattice where sites can be occupied by a susceptible host (S), an infected host (I), or be empty (O), the change in the number of paired states on the lattice (e.g., SO pairs) can be described by the following set of equations.

$$\frac{d[SS]}{dt} = 2 \cdot \frac{r}{n} \cdot Q(S|OS) \cdot [SO] - \left\{ 2 \cdot d + 2 \cdot \frac{\beta}{n} \cdot Q(I|SS) \right\} \cdot [SS] \tag{11}$$

$$\begin{aligned} \frac{d[SO]}{dt} = {} & \frac{r}{n} \cdot Q(S|OO) \cdot [OO] + d \cdot [SS] + (d + \alpha) \cdot [IS] \\ & - \left\{ d + \frac{r}{n} \cdot Q(S|OS) + \frac{\beta}{n} \cdot Q(I|OS) \right\} \cdot [SO] \end{aligned} \tag{12}$$

$$\frac{d[OO]}{dt} = 2 \cdot d \cdot [SO] + 2 \cdot (d + \alpha) \cdot [IO] + 2 \cdot \frac{r}{n} \cdot Q(S|OO) \cdot [OO] \tag{13}$$

$$\frac{d[II]}{dt} = 2 \cdot \frac{\beta}{n} \cdot Q(I|SI) \cdot [SI] - 2 \cdot (d + \alpha) \cdot [II] \tag{14}$$

$$\frac{d[IS]}{dt} = \frac{r}{n} \cdot Q(S|OI) \cdot [IO] + \frac{\beta}{n} \cdot Q(I|SS) \cdot [SS] - \left\{ 2 \cdot d + \alpha + \frac{\beta}{n} \cdot Q(I|SI) \right\} \cdot [IS] \tag{15}$$

$$\frac{d[IO]}{dt} = \frac{\beta}{n} \cdot Q(I|SO) \cdot [SO] + d \cdot [IS] + (d + \alpha) \cdot [II] - \left\{ d + \alpha + \frac{r}{n} \cdot Q(S|OI) \right\} [OI] \tag{16}$$

In these equations, r is the host reproduction rate, d is the natural host death rate, α is the pathogen virulence, β is the pathogen transmission rate, and n is the neighborhood size. $Q(X|YZ)$ is the number of lattice sites in state X in the neighborhood of a site in state Y with a neighboring lattice site in state Z. This set of equations does not incorporate any approximations but is not closed. Further, these equations can be scaled to the size of the lattice and interaction neighborhood to represent the proportion of state pairs on the lattice. Summing Eqs. 11, 12, and 15 yields an equation for the time derivative of the number of susceptible hosts on the lattice, summing Eqs. 14–16 yields the time derivative of the number of infected hosts, and summing Eqs. 12, 13, and 16 yields the time derivative of the number of empty sites.

Appendix 3

Improved pair approximation (IPA)

Equations 11–16 are not closed. Quantities involving state triples ($Q(X|YZ)$) depend on higher order state combinations. To solve these equations, a moment closure method is required. An ordinary pair approximation (OPA) simply assumes that the presence of a site in state X next to a site in state Y does not depend on the state of other sites in the neighborhood of Y. Thus,

$$Q(X|YZ) = (1 - \theta) \cdot Q(X|Y) \tag{17}$$

$$Q(X|YX) = (1 - \theta) \cdot Q(X|Y) + 1 \tag{18}$$

where θ is $1/n$ and scales the relationship to account for the fact that the maximum $Q(X|Y)$ is 4 but the maximum $Q(X|YZ)$ is 3. However, when host reproduction is local, $Q(S|OO)$ should be smaller than $Q(S|O)$ and $Q(S|OS)$ should be larger than $Q(S|O)$ because susceptible hosts will tend to cluster in space. The improved pair approximation (IPA) takes this clustering into account. When the size of the neighborhood on the lattice is 4, the ratio of $Q(S|OO)$ to $Q(S|O)$ has been shown to be approximately 0.8093. Thus, the IPA assumes that

$$Q(S|OO) = 0.89093 \cdot (1-\theta) \cdot Q(S|O) \tag{19}$$

Using the relationship in Eq. 19 and the following identity relationship

$$Q(S|OS) \cdot Q(S|O) + Q(S|OO) \cdot Q(O|O) + Q(S|OI) \cdot Q(I|O) = Q(S|O) \tag{20}$$

the IPA also assumes that

$$Q(S|OS) = n - (1-\theta) \cdot Q(I|O) - 0.89093 \cdot (1-\theta) + Q(O|O) \tag{21}$$

Appendix 4

Solving for quasi-equilibrium $Q(S|I)$

The quasi-equilibrium $Q(S|I)$ for a pathogen strain invading a resident strain in equilibrium with the host population must be obtained numerically. Using IPA, for two pathogen strains J and K, where J is the invading strain and K is the resident strain, the time derivatives of paired states involving strain J are:

$$\begin{aligned}\frac{d[I_JS]}{dt} = {} & \frac{r}{n} \cdot (1-\theta) \cdot Q(S|O) \cdot [I_JO] + \frac{\beta_J}{n} \cdot (1-\theta) \cdot Q(I_J|S) \cdot [SS] \\ & - \left\{ 2 \cdot d + \alpha_J + \frac{\beta_K}{n} \cdot Q(I_K|S) + \frac{\beta_J}{n} \cdot (1 + (1-\theta) \cdot Q(I_K|S)) \right\} \cdot [I_JS]\end{aligned} \tag{22}$$

$$\begin{aligned}\frac{d[I_JO]}{dt} = {} & \frac{\beta_J}{n} \cdot (1-\theta) \cdot Q(I_J|S) \cdot [SO] + d \cdot [I_JS] + (d+\alpha_J) \cdot [I_JI_J] + (d+\alpha_K) \cdot [I_KI_J] \\ & - \left\{ d + \alpha_J + \frac{r}{n} \cdot (1-\theta) \cdot Q(S|O) \right\} \cdot [OI_J]\end{aligned} \tag{23}$$

$$\frac{dI_JI_J}{dt} = 2 \cdot \frac{\beta_J}{n} \cdot (1 + (1-\theta) \cdot Q(I_J|S)) \cdot [SI_J] - 2 \cdot (d+\alpha_J) \cdot [I_JI_J] \tag{24}$$

$$\begin{aligned}\frac{dI_JI_K}{dt} = {} & \frac{\beta_J}{n} \cdot (1-\theta) \cdot Q(I_J|S) \cdot [SI_K] + \frac{\beta_K}{n} \cdot (1-\theta) \cdot Q(I_K|S) \cdot [SI_J] \\ & - (2 \cdot d + \alpha_J + \alpha_K) \cdot [I_JI_K]\end{aligned} \tag{25}$$

Parameters are as defined above and θ is $1/n$. Numerically solving these equations assuming equilibrium values for all pairs and $Q(X|Y)$ that do not involve strain J (e.g., in Eq. 22, $[SS]$, $Q(S|O)$, and $Q(I_K|S)$), yields the quasi-equilibrium number of state pairs for the invading pathogen. The quasi-equilibrium $Q_{S/I}$ for strain J can then be calculated as:

$$Q^0(S|I_J) = [SI_J]^0 / [I_J]^0 \tag{26}$$

Appendix 5

Supplementary data and figures

Shape of the transmission–virulence relationship

Figure 8 shows the predicted effect of the shape of the transmission–virulence relationship on the evolutionary stable (ES) transmission rate. For linear relationships (Fig. 8a), simulations and the IPA predict a decrease in the ES transmission rate with increasing relationship steepness (higher values of C in the relationship $\alpha = C{\cdot}\beta$). The non-spatial model predicts no trend with relationship steepness. The IPA predicts higher ES transmission rates than simulations and the predictions diverge for less steep relationships. For concave-down transmission–virulence tradeoffs (Fig. 8b), simulations, the IPA, and the non-spatial model all predict a decrease in the ES transmission rate with increasing tradeoff steepness (higher values of z in the relationship $\alpha = C{\cdot}\beta^z$). As with linear relationships, the IPA and non-spatial model predict higher ES transmission rates than simulations and the predictions diverge for less steep tradeoffs (Fig. 8b, lower panel).

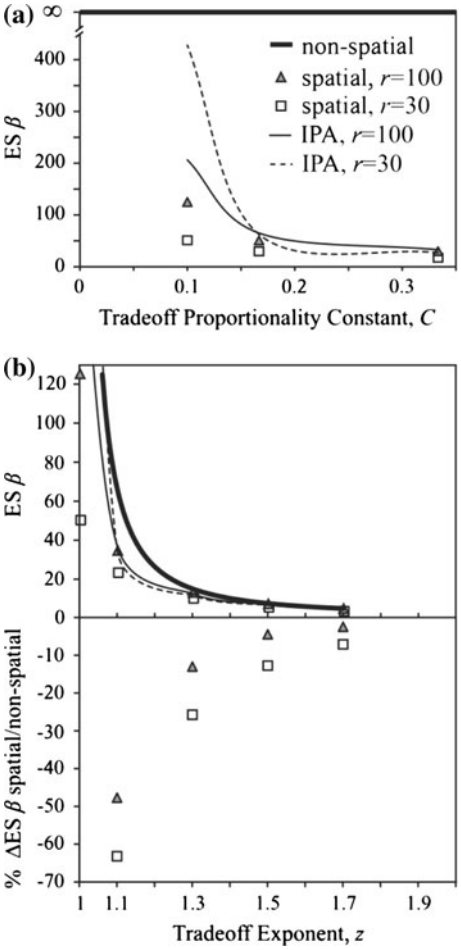

Fig. 8 ES transmission rates across transmission–virulence relationships. The ES transmission rates (ES β) obtained from simulation (data points) and predictions from improved pair approximation (IPA; *thin lines*) and a non-spatial model (*thick lines*) are shown for different transmission–virulence relationships and for two host reproduction rates ($r = 30$, *squares* and *dashed line*; $r = 100$, *triangles* and *solid line*). **a** Linear transmission–virulence relationships, shape controlled by constant of proportionality C in $\alpha = C{\cdot}\beta^z$ when $z = 1$, **b** concave-down transmission–virulence tradeoffs, shape controlled by tradeoff exponent z in $\alpha = C{\cdot}\beta^z$ when $C = 0.1$. The *top panel* shows ES β and *bottom panel* shows the percent difference between the spatial and non-spatial predictions

Host reproduction rate

Figure 9 shows the predicted effect of the host reproduction rate on the ES transmission rate for no transmission–virulence relationship across a range of natural host death rates and pathogen virulence. In particular, simulations predict that the ES transmission rate initially decreases and then increases with host reproduction rate for low host death rates ($d = 1$, $d = 2$) and pathogen virulence ($\alpha = 0$, $\alpha = 1$). For higher host death rates ($d = 3$, $d = 4$) and pathogen virulence ($\alpha = 2$, $\alpha = 3$), simulations predict that the ES transmission rate increases with host reproduction. In all cases, the non-spatial model and the IPA predict an infinite ES transmission rate (and pathogen-driven extinction) and thus no trend with host reproduction.

Figure 10 shows the predicted effect of the host reproduction rate on the ES transmission rate for linear transmission–virulence relationships. Simulations predict an increase in the ES transmission rate with the host reproduction rate. The non-spatial model predicts an infinite ES transmission rate (and pathogen-driven extinction) and thus no trend

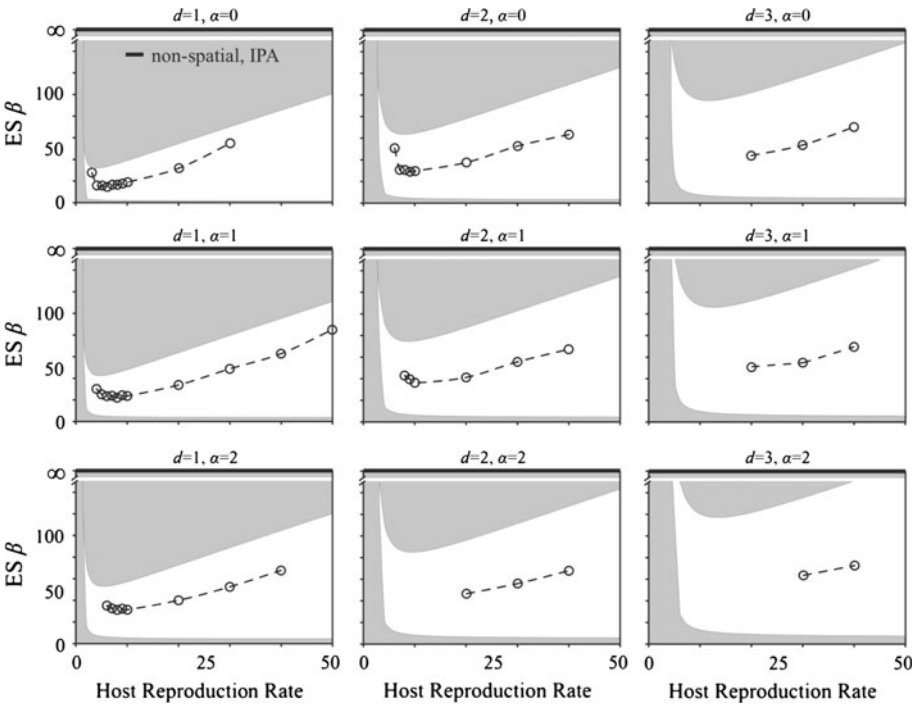

Fig. 9 Effect of host reproduction rate for no transmission–virulence relationship. The ES transmission rates (ES β) obtained from simulation (*circles with dashed spline fit*) are shown for a range of host reproduction rates, pathogen virulence, and host natural death rates along with predictions from the non-spatial model and improved pair approximation (IPA; *thick lines*). The *shaded areas* are regions where the IPA predicts extinction of the host, pathogen, or both. In the region to the left, the host will go extinct due to an insufficient reproduction rate. In the upper region the pathogen drives the host population and itself to extinction. In the lower region the pathogen cannot invade the host population due to an insufficient transmission rate. In some cases (high d or α) data could not be obtained for lower values of r, likely because the predicted invasion threshold is underestimated. For all cases, the non-spatial model and IPA predict evolution to infinite ES transmission rates and pathogen-driven extinction

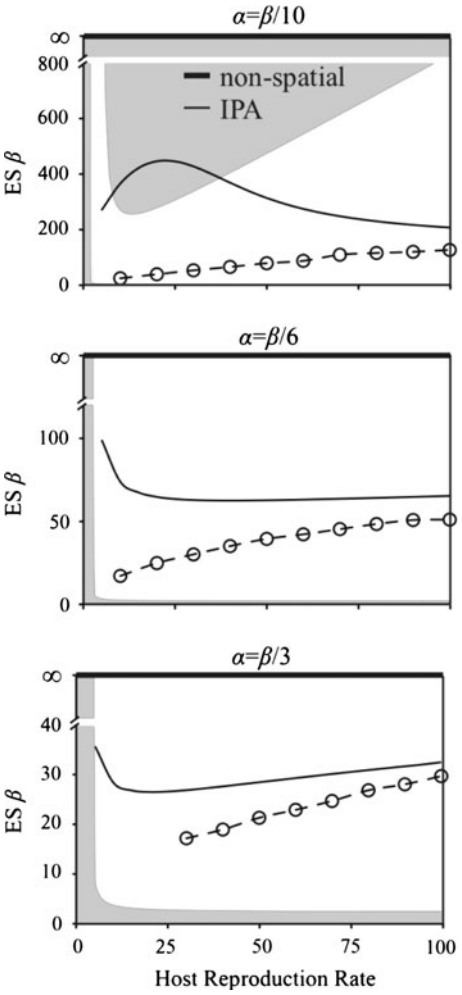

Fig. 10 Effect of host reproduction rate for linear transmission–virulence relationships. The ES transmission rates (ES β) obtained from simulation (*circles with dashed spline fit*) are shown across a range of host reproduction rates and tradeoff steepness, along with predictions from the non-spatial model (*thick solid line*) and improved pair approximation (IPA; *thin solid line*). The *shaded areas* are as in Fig. 9. Data could not be obtained for lower values of r, likely because the IPA predicted invasion threshold is underestimated. For all graphs, $d = 1$

with host reproduction. The IPA correctly predicts an intermediate ES transmission rate for all host reproduction rates. However, the trends with host reproduction are qualitatively wrong, especially when the relationship is less steep and the host reproduction rate is low: the ES transmission rate is predicted to be greater than the extinction threshold transmission rate, effectively predicting pathogen-driven extinction.

Figure 11 shows the predicted effect of the host reproduction rate on the ES transmission rate for concave-down transmission–virulence tradeoffs. Simulations predict an increase in the ES transmission rate with the host reproduction rate. Though the non-spatial model correctly predicts an intermediate transmission rate across host reproduction rates, it predicts no trend with the host reproduction rate. The IPA correctly predicts that the ES transmission rate varies with the host reproduction rate. Further, the predicted trends are qualitatively similar to the trends predicted by simulation. Quantitatively, however, the relative difference between the ES transmission rate predicted by IPA and simulations varies depending on the steepness of transmission–virulence tradeoff as well as the host

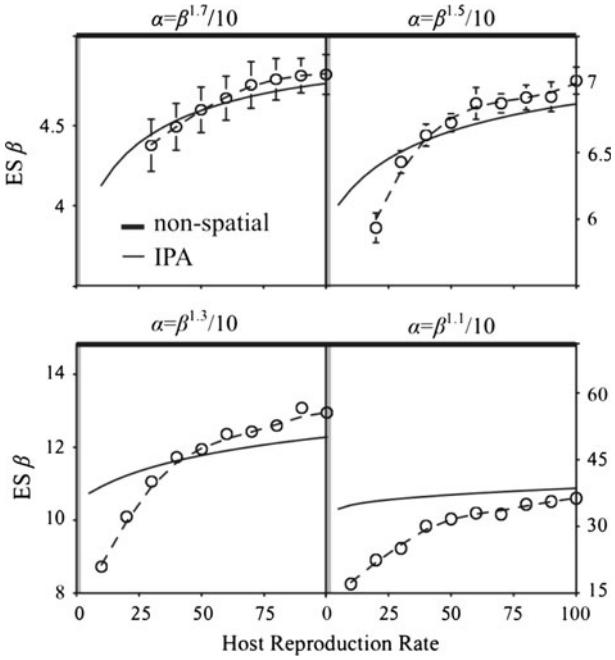

Fig. 11 Effect of host reproduction rate for concave-down transmission–virulence tradeoffs. The ES transmission rates (ES β) obtained from simulation (*circles with dashed spline fit*, *error bars* shown when larger than data points) are shown across a range of host reproduction rates and tradeoff steepness, along with predictions from the non-spatial model (*thick solid line*) and improved pair approximation (IPA; *thin solid line*). The *shaded areas* are as in Fig. 9

reproduction rate and natural death rate. As the transmission–virulence tradeoff becomes steeper (higher z in $\alpha = C{\cdot}\beta^z$ where $C = 0.1$) the relative difference decreases. In fact, for the steepest tradeoff ($\alpha = 0.1{\cdot}\beta^{1.7}$), the difference between predictions is nearly 0 across all host reproduction rates. For less steep tradeoffs, the relative difference is highest for low host reproduction rates, but decreases as host reproduction increases.

Host mortality

Figure 12 shows the effect of host mortality (either natural host death rate or virulence) on the ES transmission rate for no transmission–virulence relationship. Simulations predict that the ES transmission rate will increase with increased host mortality. However, the factor of increase declines as the host reproduction rate increases, and for high host reproduction rates the ES transmission rate may actually decrease. The non-spatial model predicts an infinite ES transmission rate for all mortality rates and thus predicts no trend with either the host natural death rate or virulence. Similarly, the IPA incorrectly predicts an infinite ES transmission rate and pathogen-driven extinction regardless of the host natural death rate or virulence. Thus, the ES transmission rate predicted by IPA is both qualitatively and quantitatively inaccurate.

Figure 13 (top two panels and lower left panel) shows the effect of host mortality (natural host death rate) on the ES transmission rate for linear transmission–virulence

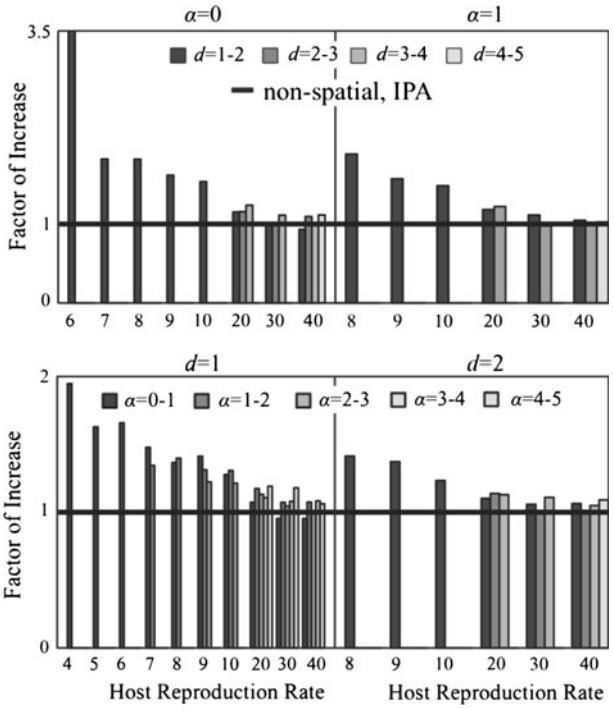

Fig. 12 Effect of host mortality on ES transmission rate for no transmission–virulence relationship. The factor of increase in the ES transmission rate (ES β) with a unit increase in the death rate (d; *top left panel* $\alpha = 0$ and *top right panel* $\alpha = 1$) and virulence (α; *bottom left panel* $d = 1$ and *bottom right panel* $d = 2$) from simulations (*bars*) along with predictions from the non-spatial model and improved pair approximation (IPA; *thick lines*) is shown for a range of host reproduction rates. A value of 1 represents no change in the ES β with death rate or virulence, a value greater than 1 is an increase, and a value less than 1 is a decrease. For example, the *first bar* in the *top left graph* (the $d = 1$–2 bar) indicates that when $\alpha = 0$ the ES transmission rate is 3.5 times higher when $d = 2$ than when $d = 1$. The non-spatial model and IPA predict no change across host reproduction rates

relationships. Simulations predict that the ES transmission rate will increase with increased host mortality. In some cases the factor of increase is greater for low host reproduction rates, but the trend is not consistent across relationship shapes. For some parameter sets the IPA correctly predicts that the ES transmission rate should increase with host death rate; however, overall the predicted trends are qualitatively and quantitatively inaccurate.

Figure 13 (lower right panel) also shows the effect of host mortality (natural host death rate) on the ES transmission rate for a concave-down transmission–virulence tradeoff. Simulations, the non-spatial model, and the IPA predict that the ES transmission rate will increase with increased host mortality. The non-spatial model predicts the same factor of increase in the ES transmission rate with host mortality across host reproduction rates. In contrast, though the trends are not strong, the IPA predicts a slight decrease in the influence of host death with host reproduction while simulations predict a slight increase with host reproduction.

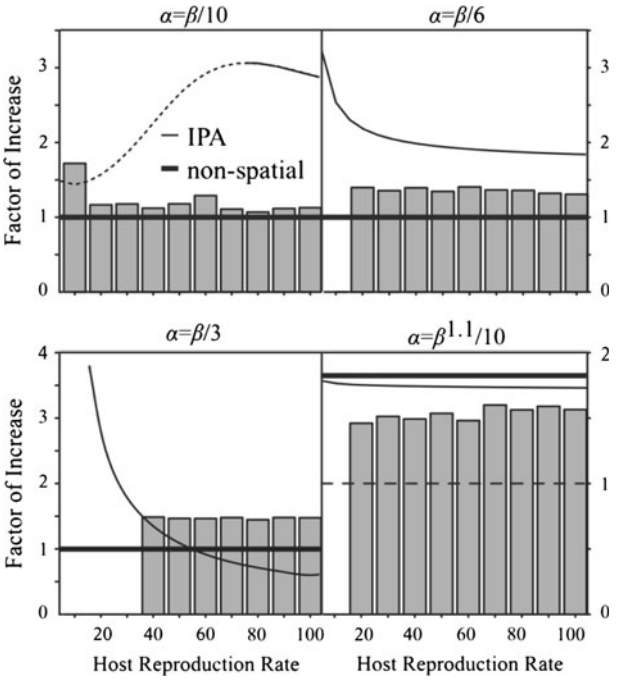

Fig. 13 Effect of host mortality on ES transmission rate for transmission–virulence relationships, linear and concave-down tradeoffs. The factor of increase in the ES transmission rate (ES β) with an increase in the death rate from $d = 1$ to $d = 2$ is shown for a range of host reproduction rates and tradeoff types: three linear and one concave down (simulation data = *bars*, predictions from non-spatial model = *thick solid line*, predictions from IPA = *thin solid line*). The factor of increase predicted by simulations is always greater than or equal to 1 (*dashed line*). For the least steep linear tradeoff, the *dotted portion* of the *curve* indicates that the IPA predicts an ES β above the extinction threshold for $d = 1$ or $d = 2$ at that host reproduction rate

References

Alizon S, Lion S (2011) Within-host parasite cooperation and the evolution of virulence. Proc R Soc Lond Ser B Biol Sci 278(1725):3738–3747

Anderson RM, May RM (1982) Coevolution of hosts and parasites. Parasitology 85:411–426

Bauch CT (2005) The spread of infectious diseases in spatially structured populations: an invasory pair approximation. Math Biosci 198(2):217–237

Best A, Webb S, White A et al (2011) Host resistance and coevolution in spatially structured populations. Proc R Soc Lond Ser B Biol Sci 278(1715):2216–2222

Boerlijst MC, van Ballegooijen WM (2010) Spatial pattern switching enables cyclic evolution in spatial epidemics. PLoS Comput Biol 6(12):e1001030

Bonhoeffer S, Lenski RE, Ebert D (1996) The curse of the pharaoh: the evolution of virulence in pathogens with long living propagules. Proc R Soc Lond Ser B Biol Sci 263(1371):715–721

Boots M, Sasaki A (1999) 'Small worlds' and the evolution of virulence: infection occurs locally and at a distance. Proc R Soc Lond Ser B Biol Sci 266(1432):1933–1938

Boots M, Sasaki A (2000) The evolutionary dynamics of local infection and global reproduction in host-parasite interactions. Ecol Lett 3(3):181–185

Boots M, Hudson PJ, Sasaki A (2004) Large shifts in pathogen virulence relate to host population structure. Science 303(5659):842–844

Boots M, Kamo M, Sasaki A (2006) The implications of spatial structure within populations to the evolution of parasites. In: Feng Z, Dieckmann U, Levin SA (eds) Disease evolution: models, concepts, and data analyses. American Mathematical Society, Providence, p 297

Bull JJ (1994) Virulence. Evolution 48(5):1423–1437
Caraco T, Glavanakov S, Li SG et al (2006) Spatially structured superinfection and the evolution of disease virulence. Theor Popul Biol 69(4):367–384
Claessen D, de Roos AM (1995) Evolution of virulence in a host-pathogen system with local pathogen transmission. Oikos 74(3):401–413
Cooper VS, Reiskind MH, Miller JA et al (2002) Timing of transmission and the evolution of virulence of an insect virus. Proc R Soc Lond Ser B Biol Sci 269(1496):1161–1165
Day T (2002) Virulence evolution via host exploitation and toxin production in spore-producing pathogens. Ecol Lett 5(4):471–476
Day T (2003) Virulence evolution and the timing of disease life-history events. Trends Ecol Evol 18(3):113–118
de Aguiar MAM, Rauch EM, Bar-Yam Y (2004) Invasion and extinction in the mean field approximation for a spatial host-pathogen model. J Stat Phys 114(5/6):1417–1451
de Roode JC, Yates AJ, Altizer S (2008) VIrulence–transmission trade-offs and population divergence in virulence in a naturally occuring butterfly parasite. PNAS 105(21):7489–7494
Dieckmann U, Law R (2000) Moment approximations of individual-based models. In: Dieckmann U, Law R, Metz JAJ (eds) The geometry of ecological interactions: simplifying spatial complexity. Cambridge University Press, Cambridge, pp 252–270
Eshelman CM, Vouk R, Stewart JL, Halsne E, Lindsey HA, Schneider S, Gualu M, Dean AM, Kerr B (2010) Unrestricted migration favours virulent pathogens in experimental metapopulations: evolutionary genetics of a rapacious life history. Phil Trans R Soc B Biol Sci 365(1552):2503–2513
Ewald PW (1987) Transmission modes and evolution of the parasitism-mutualism continuum. Ann NY Acad Sci 503:295–306
Ewald PW (1993) Evolution of virulence. Sci Am 268:56–62
Ewald PW (1998) The evolution of virulence and emerging diseases. J Urban Health Bull NY Acad Med 75(3):480–491
Filipe JAN, Maule MM (2003) Analytical methods for predicting the behaviour of population models with general spatial interactions. Math Biosci 183(1):15–35
Frank SA (1996) Models of parasite virulence. Q Rev Biol 71(1):37–78
Gandon S (1998) The curse of the pharaoh hypothesis. Proc R Soc Lond Ser B Biol Sci 265(1405): 1545–1552
Gillespie DT (1977) Exact stochastic simulation of coupled chemical reactions. J Phys Chem 81(25): 2340–2361
Goodnight C, Rauch E, Sayama H et al (2008) Evolution in spatial predator-prey models and the "prudent predator": the inadequacy of steady-state organism fitness and the concept of individual and group selection. Complexity 13(5):23–44
Hansen SK, Rainey PB, Haagensen JAJ et al (2007) Evolution of species interactions in a biofilm community. Nature 445(7127):533–536
Harada Y, Iwasa Y (1994) Lattice population-dynamics for plants with dispersing seeds and vegetative propagation. Res Popul Ecol 36(2):237–249
Haraguchi Y, Sasaki A (2000) The evolution of parasite virulence and transmission rate in a spatially structured population. J Theor Biol 203(2):85–96
Johnson CR, Boerlijst MC (2002) Selection at the level of the community: the importance of spatial structure. Trends Ecol Evol 17(2):83–90
Johnson CR, Seinen I (2002) Selection for restraint in competitive ability in spatial competition systems. Proc R Soc Lond Ser B Biol Sci 269:655–663
Kamo M, Boots M (2004) The curse of the pharaoh in space: free-living infectious stages and the evolution of virulence in spatially explicit populations. J Theor Biol 231(3):435–441
Kamo M, Boots M (2006) The evolution of parasite dispersal, transmission, and virulence in spatial host populations. Evol Ecol 8(7):1333–1347
Kamo M, Sasaki A, Boots M (2007) The role of trade-off shapes in the evolution of parasites in spatial host populations: an approximate analytical approach. J Theor Biol 244(4):588–596
Kerr B, Godfrey-Smith P (2002) Individualist and multi-level perspectives on selection in structured populations. Biol Philos 17(4):477–517
Kerr B, Neuhauser C, Bohannan BJM et al (2006) Local migration promotes competitive restraint in a host-pathogen 'tragedy of the commons'. Nature 442(7098):75–78
Le Galliard JF, Ferriere R, Dieckmann U (2003) The adaptive dynamics of altruism in spatially heterogeneous populations. Evolution 57(1):1–17
Levin BR, Bull JJ (1994) Short-sighted evolution and the virulence of pathogenic microorganisms. Trends Microbiol 2(3):76–81

Levin S, Pimentel D (1981) Selection of intermediate rates of increase in parasite-host systems. Am Nat 117(3):308–315
Lion S, Boots M (2010) Are parasites ''prudent'' in space? Ecol Lett 13(10):1245–1255
Lion S, van Baalen M (2008) Self-structuring in spatial evolutionary ecology. Ecol Lett 11(3):277–295
Matsuda H, Ogita N, Sasaki A et al (1992) Statistical mechanics of population: the lattice Lotka-Volterra model. Prog Theor Phys 88(6):1035–1049
May RM, Anderson RM (1982) Parasite-host coevolution. In: Futuyma DJ, Slatkin M (eds) Coevolution. Sinauer Associates, Inc., Sunderland, pp 186–206
Messinger SM, Ostling A (2009) The consequences of spatial structure for the evolution of pathogen transmission rate and virulence. Am Nat 174(4):441–454
Morris AJ (1997) Representing spatial interactions in simple ecological models. Dissertation, University of Warwick
Mosquera J, Adler FR (1998) Evolution of virulence: a unified framework for coinfection and superinfection. J Theor Biol 195(3):293–313
Nowak MA, Sigmund K (2002) Super- and coinfection: the two extremes. In: Dieckmann U, Metz JAJ, Sabelis MW, Sigmund K (eds) Adaptive dynamics of infectious diseases: in pursuit of virulence management. Cambridge University Press, Cambridge, pp 124–149
Ohtsuka K, Konno N, Masuda N et al (2006) Phase diagrams and correlation inequalities of a three-state stochastic epidemic model on the square lattice. Int J Bifurc Chaos 16(12):3687–3693
Osnas EE, Dobson AP (2010) Evolution of virulence when transmission occurs before disease. Biol Lett 6(4):505–508
Peyrard N, Dieckmann U, Franc A (2008) Long-range correlations improve understanding of the influence of network structure on contact dynamics. Theor Popul Biol 73(3):383–394
Prado F, Kerr B (2008) The evolution of restraint in bacterial biofilms under nontransitive competition. Evolution 62(3):538–548
Rauch EM, Sayama H, Bar-Yam Y (2002) Relationship between measures of fitness and time scale in evolution. Phys Rev Lett 88(22):1–4
Roche B, Drake JM, Rohani P (2011) The curse of the Pharaoh revisited: evolutionary bi-stability in environmentally transmitted pathogens. Ecol Lett 14(4):569–575
Sato K, Matsuda H, Sasaki A (1994) Pathogen invasion and host extinction in lattice structured populations. J Math Biol 32(3):251–268
Slobodkin LB (1974) Prudent predation does not require group selection. Am Nat 108(963):665–678
van Baalen M, Rand DA (1998) The unit of selection in viscous populations and the evolution of altruism. J Theor Biol 193(4):631–648
van Baalen M, Saebelis MW (1995) The milker-killer dilemma in spatially structured predator–prey interactions. Oikos 74:391–400
Walther BA, Ewald PW (2004) Pathogen survival in the external environment and the evolution of virulence. Biol Rev 79(4):849–869
Webb SD, Keeling MJ, Boots M (2007a) Spatially extended host-parasite interactions: the role of recovery and immunity. Theor Popul Biol 71(2):251–266
Webb SD, Keeling MJ, Boots M (2007b) Host–parasite interactions between the local and the non-spatial: how and when does spatial population structure matter? J Theor Biol 249(1):140–152
White PJ, Norman RA, Hudson PJ (2002) Epidemiological consequences of a pathogen having both virulent and avirulent modes of transmission: the case of rabbit haemorrhagic disease virus. Epidemiol Infect 129(3):665–677